

A comparative study of optical fibre types for application in a laser-induced ignition system

J D Mullett¹, G Dearden¹, R Dodd¹, A T Shenton², G Triantos² and K G Watkins¹

¹ Laser Group, Department of Engineering, University of Liverpool, Brownlow Street, Liverpool L69 3GH, UK

² Powertrain Control Group, Department of Engineering, University of Liverpool, Brownlow Street, Liverpool L69 3GH, UK

E-mail: jmullett@liv.ac.uk

Received 30 September 2008, accepted for publication 19 November 2008

Published 18 March 2009

Online at stacks.iop.org/JOptA/11/054007

Abstract

Various types of optical fibres have been investigated and compared for delivering high power laser beams to an optical plug (comprising of lenses and an optical window) for the application of laser-induced ignition of gasoline and air mixtures in an automotive internal combustion engine. Three main types of optical fibre were examined: multi-mode step index silica, sapphire and photonic crystal. The fibres had various core sizes ranging from 35 to 600 μm and numerical apertures between 0.046 and 0.64. A Q-switched Nd:YAG laser operating at the fundamental wavelength 1064 nm with a pulse length of 15 ns was used for the testing. Fibre output beam properties, including beam mode quality, output divergence, transmission losses, beam energy thresholds and effects of engine vibration were investigated. These fibre beam properties were compared with known beam parameters for laser ignition to assess the suitability of such fibres for a laser ignition system. Online fibre delivery laser ignition engine tests were performed with the most suitable fibres, which showed that combustion could be achieved with this system despite a relatively large percentage of misfires.

Keywords: optical fibre beam delivery, laser ignition, gasoline IC engine

(Some figures in this article are in colour only in the electronic version)

1. Introduction

Laser-induced ignition (LI) of air–fuel mixtures in internal combustion (IC) engines has many potential advantages over conventional electrical spark ignition (SI). These benefits include: variable ignition positions within a cylinder/combustion chamber [1], absence of electrodes which can disturb the cylinder geometry and can quench a propagating flame kernel [2], possibility of multiple ignition positions in time and space [3, 4], lower ignition energies [5], more stable combustion [5, 6], reduced tailpipe emissions [7] and combustion of leaner air–fuel mixtures [6].

There are four principle LI mechanisms: non-resonant breakdown ignition, resonant breakdown ignition, thermal

ignition and photochemical ignition [8]. The most widely used mechanism is non-resonant breakdown as this is most similar to conventional electric SI, in that a plasma is produced which emits light, heat and a shockwave. However, laser-induced sparks are generally smaller in size, shorter in duration and have higher temperatures and densities [9]. For non-resonant breakdown, a laser beam must be sufficiently focused to produce laser irradiances in excess of $10^{11} \text{ W cm}^{-2}$ at the minimum beam waist. Here, the electrical field of the focused beam is sufficient to cause dielectric breakdown of the air–fuel mixture. The process generally begins with multi-photon ionization of a few molecules, which leads to the release of electrons that can then readily absorb more photons from the laser source via the inverse bremsstrahlung process. This in

turn increases the kinetic energy of these released electrons, which then collide with other molecules and ionize them, leading to an electron avalanche and subsequent breakdown of the combustible gas mixture [2, 8, 10].

Open beam path optical arrangements have been used for the majority of LI research, and although this is suitable for laboratory experiments, it is not appropriate for real-world use. Therefore, if LI is to become a commercially viable alternative to spark plugs in the future, a practical, inexpensive, reliable and robust beam delivery method must first be developed. Possible solutions to this could be to have individual compact lasers combined with an optical plug for each cylinder [11], or to have a single laser with the beam split and coupled into fibres to deliver the beams to optical plugs located in each cylinder [12]. The latter has the advantage of having the laser source remote from the harsh engine environment. A third potential solution is a hybrid of the first two, which is the use of fibre lasers for each engine cylinder. However, at present they do not have high enough output beam energies required for ignition, although the technology is advancing at a rapid rate.

Optical fibre laser delivery using common multi-mode step index fibres is well established in areas such as laser material processing (laser drilling, cutting and welding) for delivering high beam energies to a work piece. However, to produce a laser-induced spark in air at atmospheric pressure with a beam that has been delivered by an optical fibre is much more technically challenging. The main reason for this is that the damage threshold of conventional silica fibre ($\approx 5 \text{ GW cm}^{-2}$) is an order of magnitude lower than the laser irradiance required to produce a spark (optical breakdown) in air, which is $> 100 \text{ GW cm}^{-2}$ [13]. Also, the beam exiting a multi-mode optical fibre will be of a poorer beam quality (higher M^2) compared to the input beam, as many modes become excited as the beam propagates through the fibre. This reduces the fibre output beams' focusability to produce a small beam spot required for optical breakdown. Therefore, the aim of the research presented in this paper is to compare and assess the suitability of various optical fibres for beam delivery in an LI system and investigate methods for increasing the deliverable beam energy and retaining fibre output beam quality.

To date, the only demonstration of a laser-induced spark at atmospheric pressure by optical fibre delivery has been performed by Yalin *et al* [14]. They used a cyclic olefin-polymer-coated $700 \mu\text{m}$ hollow core waveguide with a silver inner coating layer developed by Matsuura *et al* [15]. This was used in subsequent research to laser-ignite natural gases in stationary reciprocating gas engines [12] using fibre output beam energies of 27 mJ and focal point laser irradiances of 100 GW cm^{-2} .

Optical breakdown at atmospheric pressure by fibre beam delivery is not necessarily required for LI of gasoline and air (or other gas) mixtures. This is because automotive engine cylinder pressures can be up to 10 bar at the time of ignition, meaning that less laser intensity is needed for combustion.

There have been relatively few studies on the investigation of optical fibres for the application of LI [12, 14, 16–18].

The majority of these studies have discarded the use of solid core optical fibres due to their damage thresholds being lower than the ignition irradiance and their poor output beam quality. However, solid core fibre-delivered LI has been demonstrated in research performed by El-Rabii and Gaborel [16]. In their work, they show preliminary results on the ignition of n-heptane and JP-4 mixtures initiated by a laser delivering nanosecond pulses of 30 mJ focused to a spot of $200 \mu\text{m}$ through a solid core silica optical fibre.

When considering the potential use of silica fibres for LI, there are two conflicting issues. The first being that due to the high beam energies involved with LI, larger core diameter fibres are preferable in order to reduce the associated laser irradiances which can damage the fibre. However, in order to focus the fibre output beam to a sufficiently small spot to obtain the required irradiance needed for ignition, a smaller fibre core diameter is desirable, as this produces an output beam with less modes and better beam quality.

There are also certain physical design constraints when designing a fibre-delivered LI system for an automotive engine. The main ones are the size of the access hole into an engine's cylinder currently taken up by the spark plug (which can vary depending on the engine) and the severe heat and vibration ranges caused by the engine. These issues and concerns are addressed in the following sections.

2. Experimental set-up and procedure

The general experimental set-up for the optical fibre testing is illustrated in figure 1. The laser used for the experiments was a 'Mini-Q' flashlamp-pumped Q-switched pulsed Nd:YAG laser, manufactured by GSI Group, which operated at the fundamental wavelength 1064 nm. The laser originally had a pulse width of 5 ns. However, for these optical fibre experiments, the laser cavity was lengthened from 0.5 to 1.5 m, which extended the pulse length to 15 ns, which was measured to the full width at half-maximum (FWHM). This was performed in order to reduce the thermal impact on the optical components and hence increase the energy damage thresholds of the fibres investigated.

The laser's internal cavity aperture was removed for the majority of the fibre testing, resulting in a multi-mode output beam profile and energies of up to 180 mJ per beam pulse. The output beam divergence was found to be 10 mrad using a laser beam analyser (LBA) system (Electrophysics 'Micro-viewer' 7290A charge-coupled device camera and software), where the cross-sectional beam sizes were measured to the $1/e^2$ limit (86.5% of beam) to an accuracy of $\pm 5 \mu\text{m}$. The LBA was also used to find the beam quality factor, M^2 , which was calculated to be 5.2 using equation (1):

$$d_M = \frac{4M^2 f \lambda}{\pi d_L} \quad (1)$$

where d_M is the minimum beam spot diameter, f is the focal length of the focusing lens, λ is the laser beam wavelength and d_L is the beam diameter incident on the focusing lens.

An exception to the above-mentioned laser configuration was for the examination of the large mode area (LMA)

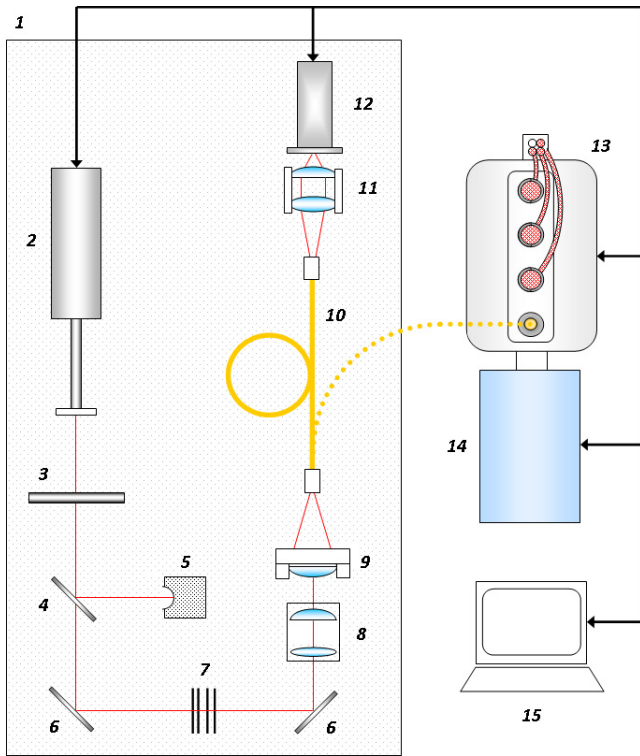


Figure 1. Experimental set-up for optical fibre testing: (1) optical bench, (2) Nd:YAG laser with extended cavity, (3) variable polarizer, (4) 1/4-wave plate, (5) beam dump, (6) neutral density filters, (7) mirror, (8) variable telescope, (9) fibre launch lens, (10) optical fibre, (11) fibre output optics (optical plug), (12) CCD camera/energy meter, (13) 1.6 L Zetec IC engine, (14) low inertia dynamometer and (15) control and data acquisition PC.

photonic crystal fibre, where a 1.4 mm diameter aperture was used in the laser cavity to produce a near-Gaussian TEM₀₀ mode intensity beam profile. This was necessary as the fibre required a single-mode input beam in order to focus the beam down to the small core size of 35 μm with a shallow fibre launch angle. For this laser configuration, the M^2 and output beam divergence were calculated to be 1.5 and 4 mrad, where the maximum pulse energy was 20 mJ.

Due to the nature of lasers, output beam properties tend to change with varying pulse energies and repetition rates. This is due to a phenomenon known as thermal lensing, where a lensing effect occurs in the laser crystal (or gain medium). This effect is particularly apparent for flashlamp-pumped lasers, which were used for these experiments. As the flashlamp (or pumping medium) is driven harder and quicker by increased beam frequency and energy, a thermal gradient is produced across the cross section of the laser crystal. This causes the refractive index of the crystal to change, thereby affecting the output beam. When a beam is focused by a lens (or number of lenses), then the diameter of the minimum beam waist produced is a function of the beam diameter incident on the focusing lens, as shown in equation (1). Therefore, if the output laser beam were to increase in size with increased energy or repetition rate, then the focused minimum beam spot would become smaller. This would cause the laser irradiance (W cm⁻²) at this point to increase and therefore could cause the damage threshold of the fibre to be exceeded.

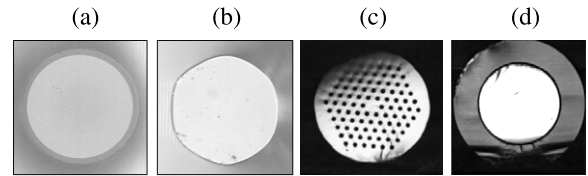


Figure 2. Microscope images of optical fibre ends: (a) silica step index fibre, (b) sapphire fibre, (c) large mode area photonic crystal fibre and (d) multi-mode ultra-high numerical aperture photonic crystal fibre.

To reduce the effects of this issue, a variable polarizer, 1/4-wave plate and beam dump were positioned at the laser output in the set-up, as illustrated in figure 1. The laser was driven at 90% power for all experiments. The beam energy was adjusted by rotating the beam's plane of polarization, where the 1/4-wave plate would reflect a portion of the beam into a beam dump (or onto an energy meter) and transmit the remaining through.

To ensure that the same beam angles were launched into the fibres, a variable telescope was used in the experimental set-up before the optical fibre and launching lens, as shown in figure 1. Various singlet lenses with different focal lengths (−50–400 mm) were used in the telescope and for launching the beam into the fibre, to achieve a wide range of fibre input beam angles.

Three main types of optical fibre were investigated for the application of LI: multi-mode step index silica fibres, sapphire fibres and photonic crystal fibres (PCF), where the choice was largely due to availability. All these fibres were 1 m in length and had various core sizes ranging from 35 to 600 μm, with numerical apertures (NA) between 0.046 and 0.64. The details of the specific fibres tested are shown in table 1 and the ends of the different fibre types can be seen in figure 2. The silica and sapphire optical fibre ends were prepared by hand using the lap and polish method and the PCF ends were prepared by the manufacturer.

A cross-sectional beam diameter of approximately 90% of the fibre core diameter was launched into all the optical fibres. For example, a fibre with a core diameter of 600 μm would have a 540 μm beam diameter, measured to the 1/*e*² limit, launched into the fibre. The focused minimum beam waist created by the fibre launch optics was located before the input fibre face, so that the beam started to diverge as it entered the fibre. This is common practice with high power fibre beam delivery in order to prevent damage to the fibre [19, 20].

The fibre output optical assembly consisted of a dual-lens imaging system, which is illustrated in figure 3. Various singlet lenses made of BK7 were used, which had focal lengths ranging from 9 to 45 mm.

When the optics are arranged in this way (figure 3), the minimum focused beam spot diameter, d_s , is a function of the fibre core diameter, d_c , and the ratio of the focal lengths of the two lenses, L_1 and L_2 , and can be calculated using equation (2):

$$d_s = \frac{d_c L_2}{L_1}. \quad (2)$$

Table 1. Details of the various optical fibres tested.

Optical fibre type		Core diameter (μm)	Cladding diameter (μm)	Buffer diameter (μm)	NA	Manufacturer
Pure silica—step index		200	240	320	0.12	CeramOptec
		200	230	400	0.22	3M
		200	225	400	0.48	3M
		300	330	430	0.22	GSI group
		365	400	730	0.22	3M
		365	400	730	0.48	3M
		400	440	540	0.12	CeramOptec
		400	440	540	0.22	CeramOptec
		400	425	730	0.48	3M
		600	660	760	0.12	CeramOptec
	600	660	760	0.22	CeramOptec	
Sapphire		250	—	—	0.12	Laser components
		325	—	—	0.12	Laser components
Photonic crystal (silica)	LMA	35	283	—	0.046	Crystal fibre A/S
	MM.UH.NA	112	229	—	0.64	
		200	335	—	0.64	

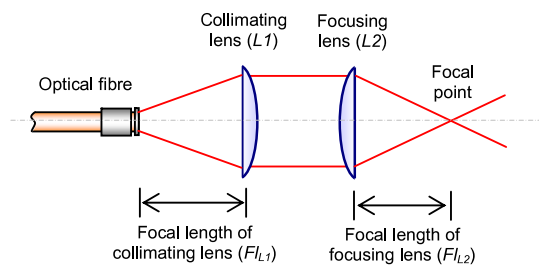


Figure 3. Fibre output optical assembly used in the fibre-delivered laser ignition system.

Four different sets of experiments were performed on all the optical fibres and are described in the following subsections.

2.1. Investigation of fibre damage thresholds

These tests were conducted offline on the optical bench. Firstly, an energy meter (Gentec ED200 head and Solo PE monitor) was used before and after the fibres to measure their transmission. For the duration of the fibre damage threshold testing, a straight length of fibre was used where the energy meter was positioned at approximately 50 mm from the fibre output, and the beam pulse repetition rate was kept constant at 10 Hz. The tests were started with a low input beam energy, which was gradually increased using the variable polarizer and 1/4-wave plate, until catastrophic failure of the fibre occurred. This process was repeated twice more for each fibre and an average damage energy threshold was recorded.

2.2. Investigation of fibre output beam mode and divergence

For the application of LI, lower output beam divergences from fibres are advantageous. This is due to the limited size of the spark hole in the engine cylinder, and the fact that smaller minimum beam spot sizes can be achieved with larger distances between the fibre output and the first lens in the optical plug, as shown by equation (2). Therefore, the angles at

which the laser beam was focused into the fibres were reduced from the fibre’s NA, which were compared with the fibre output beam angles. A low energy beam was used, which was well below the damage threshold of the fibre. The LBA was used to measure the cross-sectional beam diameters and also to capture the fibre output beam mode intensity profiles from all the fibres.

2.3. Effects of bending and engine vibration on fibre output properties

A shallow fibre input beam angle of 4 mrad and 5 mJ energy was used for both the fibre bending and engine vibration tests. Initially for the bending testing, a straight length of fibre was examined and used as a benchmark. A single ‘loop’ of 360° was then introduced in the fibre where its diameter was varied from a maximum of 280 mm, down to the minimum bend diameter, which was different for each fibre. The fibre bending experiments were taken further to include the effects of vibration from the running engine to give more realistic results in terms of output beam divergence. Therefore, the fibre was given a bend and a twist from the horizontal optical bench to the vertical plane, where the fibre output end was mounted on a section of the test engine, replicating the set-up for online fibre delivery LI testing. The LBA camera was mounted vertically at the fibre output to capture the beam profiles, with and without the engine vibration, at various distances from the output face. The fibre output beam divergences, intensity profiles and transmissions were recorded for both the bending and engine vibration testing.

2.4. Fibre-delivered LI engine testing

An optical plug was designed and manufactured for the online fibre-delivered LI engine testing. Various photographs of this optical plug are shown in figure 4, alongside a conventional spark plug. The optical plug allowed different configurations of two lenses to collimate and refocus the beam from a fibre into one of the test engine cylinders. Various focal length lenses were used (which were dependent on the fibre) which



Figure 4. Photographs of the optical plug: disassembled, with optical fibre attached and compared with a conventional spark plug.

were made from uncoated BK7 and had diameters of 6 mm. An uncoated sapphire window of 5 mm diameter and 1 mm thickness was used at the base of the plug to seal off the cylinder.

The IC engine used for the testing was from a Ford Mondeo. This was an unmodified four-stroke 1.6 litre aspirated port fuel-injected Zetec engine, which had four inline cylinders, 16 valves controlled by double overhead camshafts, and was operated in a homogeneous ignition mode. The single-fibre optical plug was used in one cylinder of the test engine, while the remaining three cylinders used conventional spark plugs to ignite the fuel. The laser was controlled through a dSpace DS1005 card in a bus-linked expansion box using an open-loop Simulink laser timing model designed and run through MATLAB, which ensured that the laser fired at the same time as the spark plugs. Cylinder pressure data was collected from all four cylinders, using Kistler pressure sensors *in situ* every 1° of crank angle.

3. Results and discussion

3.1. Investigation of fibre damage thresholds

Initially for the fibre damage threshold experiments, the silica step index fibre ends were permanently fixed into SMA fibre connectors (screw coupling) using adhesive, which is common practice for industrial laser set-ups. The damage thresholds for these silica fibres, in terms of laser irradiance required to cause catastrophic failure, were found to be $\approx 3 \text{ GW cm}^{-2}$. The failure point always occurred at the input fibre face, where surface cracks and expulsion of silica transpired. Compared to the laser irradiances required for LI, this damage threshold was considered too low. Therefore, in an attempt to increase the damage thresholds, the fibre ends were left free-standing in an SMA connector with a 100 mm long metal ferrule attached. The fibres were lightly clamped at the opposite end to the SMA connector on the ferrule, which is shown in figure 5.

The free-standing fibre ends made a difference to the amount of beam energy that could be delivered by the silica fibres and to the position where fibres failed. On average, the silica fibre damage thresholds increased by at least a factor of 3, to approximately 9 GW cm^{-2} . Similar observations have been shown by Allison *et al* [21], who used a similar method to clamp fibre ends. They found that the free-standing ends increased the damage threshold by reducing the stresses at the fibre face.

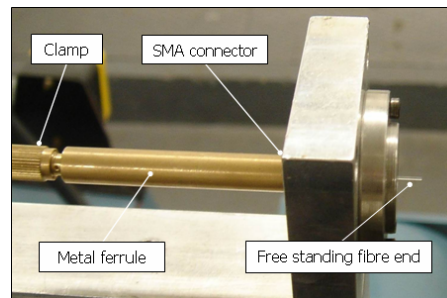


Figure 5. Free-standing fibre end ferrule holder with SMA connector.

For the free-standing fibre ends, catastrophic fibre failure was found to occur not at the input face, as was observed with the fixed connectors, but at various distances along the fibre from the input face. This is due to the fact that, when the beam is launched into the fibre, the fibre end is suddenly exposed to an extremely high heat input, which causes slight expansion of the fibre. This induces higher stresses on the fibres with the constricted adhesive fixed connectors, causing catastrophic failure at the input face. However, with the free-standing fibre ends, the fibre is not constrained and therefore the failure point was further along the fibre. The distances from the fibre input to the point of failure were found to be dependent on the input beam angle launched into the fibre, where the shallower the input beam angle, the larger the distance from the fibre input face to the point of failure. This effect is due to heat build-up at the first internal reflection within the fibre. As the free-standing fibre ends were found to increase the damage thresholds of the silica fibres, this method was used for the remainder of the experiments.

The damage thresholds for both PCF types (LMA and MM.UH.NA) were found to be slightly lower than the solid core step index silica fibres at $\approx 7 \text{ GW cm}^{-2}$. However, the failure mode was in a similar manner to the silica step index, where the fibre failed at a distance from the end of the fibre input face. The lower damage threshold of the PCFs was thought to be due to the air holes running through them, producing a different damage mechanism to that of bulk silica, where the laser radiation induces heating and creates non-uniform strains which break the thin walls of the micro-structure. Similar observations have been reported in work on damage thresholds of PCFs performed by Michaille *et al* [22].

The sapphire fibres were found to have the lowest damage thresholds of $\approx 4 \text{ GW cm}^{-2}$, of the three main types of optical fibre tested. This was thought to be due to the wavelength of the laser used (1064 nm), as the sapphire fibre is more suited for the Er:YAG laser wavelength of 2940 nm, where the attenuation is 0.2 dB m^{-1} compared to 0.4 dB m^{-1} at 1064 nm.

An interesting observation of the sapphire fibre damage threshold testing with free-standing fibre ends was that damage was only ever noticed at the input face, where continuous plasmas formed at the maximum damage threshold beam energies. Subsequent inspection of the fibre input face under a microscope showed a 'bubbled' texture on the surface where the incoming beam had irradiated, which can be seen in

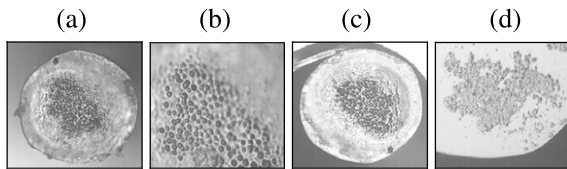


Figure 6. Microscope images of the sapphire fibre input face after damage threshold testing (a) 250 μm core diameter, (b) 250 μm core diameter, (c) 325 μm core diameter and (d) 325 μm core diameter.

figure 6. This indicates that the beam had begun to melt the sapphire surface, which has a melting temperature of 2053 °C, which caused plasmas to occur for subsequent beam pulses.

Other techniques and methods to increase the damage thresholds of fibres have been investigated by other researchers. These include CO₂ laser annealing of the fibre ends [23], air evacuation (partial vacuum) at the fibre launch and filling hollow core fibres with inert gases. Although these methods have been shown to be effective, the latter two are not really suitable for a fibre-delivered LI system as this would increase the complexity and cost. The CO₂ laser annealing of fibre ends may have merit as this was found to increase the damage threshold by an order of magnitude. This would be beneficial for fibres used in a LI system, as they would have to last for long periods without damage.

3.2. Investigation of fibre output beam mode and divergence

As expected, the 35 μm core diameter LMA PCF had the greatest output beam mode quality of all the tested fibres. A fibre output beam intensity profile measured at 35 mm from the fibre exit can be seen in figure 7, which shows the beam to be near single mode. However, the maximum beam energy that this fibre could transmit was 0.4 mJ, which is 10 times less than the minimum LI energy required for combustion of gasoline and air mixtures of similar beam quality, which is ≈4 mJ [5].

As this fibre had the smallest NA of 0.046, it was quite difficult to achieve input beam angles lower than this. Therefore, the output divergence angle was equal to the NA which equates to a half-angle of 46 mrad using equation (3), where θ_{Max} is the maximum fibre beam angle of acceptance:

$$NA = \text{Sin} \left(\frac{\theta_{Max}}{2} \right). \quad (3)$$

The fibre output beam angles from the larger multi-mode fibres were found to be dependent on the input beam angle, bends in the fibre and the fibre’s NA. The former is illustrated in figure 8, which shows the output beam divergence from a 365 μm core silica fibre of 0.22 NA for various beam input angles. This shows that smaller output beam divergence angles can be achieved with shallower fibre beam input angles, and hence greater fibre exit beam quality (lower M^2) can be obtained. This is beneficial for the application of fibres in LI as smaller focal spot sizes can be achieved within the size constraints of the engine cylinder access hole.

In theory, the beam angle focused into a straight length of fibre with end faces perpendicular to its axis should be equal

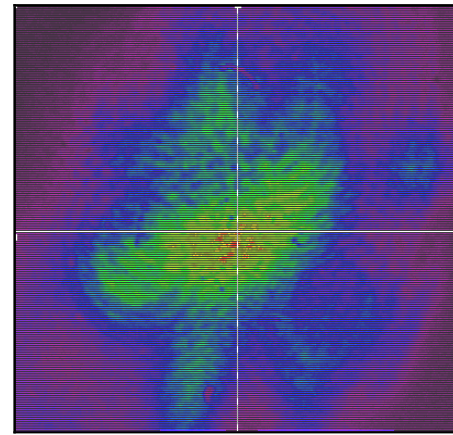


Figure 7. Beam intensity profile at 35 mm from the output of the 35 μm core LMA PCF, measured to have a 1.7 mm diameter.

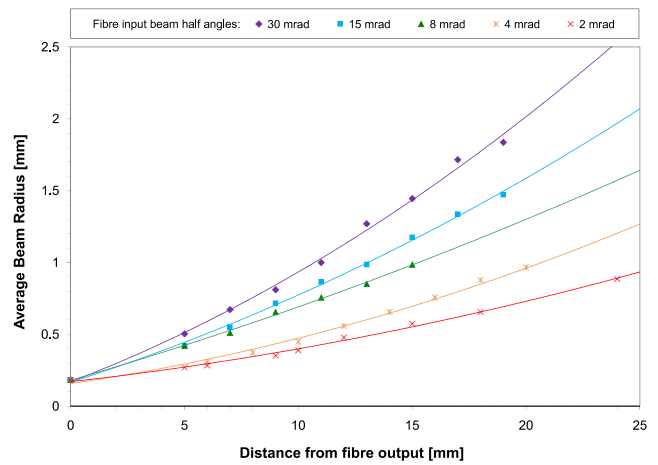


Figure 8. Output beam divergence from a 1 m straight length of 365 μm core diameter step index silica fibre of 0.22 NA with varying fibre input beam half-angles.

to the output beam angle. However, in reality, the fibre has manufacturing defects and micro-bends which cause the exit beam angle to be larger. A relationship was found between the input and output angles for straight lengths of silica fibre, where the output beam angles were approximately 2.5 times that of the input angles.

The transmission losses of the step index silica fibres were calculated to be ≈8%, which was as expected, as approximately 4% of the beam is reflected at both the entrance and exit faces of the fibre. The transmission losses of the sapphire fibres were higher at ≈20%, which again was expected as this was the transmission quoted by the manufacturer at the 1064 nm wavelength.

3.3. Effects of bending and engine vibration on fibre output properties

The output beam divergence of a 400 μm core silica of 0.22 NA and 1 m length with different bend diameters introduced into the fibre is shown in figure 9. It is evident that reducing the bend diameter in the fibre increases the output beam divergence

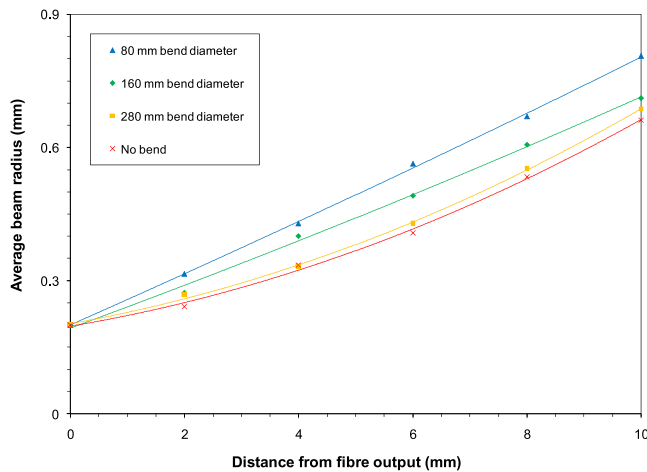


Figure 9. Output beam divergence from a 1 m length of 400 μm core diameter step index silica fibre of 0.22 NA with various bend diameters in the fibre.

until it reaches the NA of the fibre, which therefore reduces the fibre output beam quality. Similar observations were seen in work by Kuhn *et al* [24]. This was found to be true for all the step index fibres, although the smaller the fibre core, the less the sensitivity to bends. In addition, the higher NA fibres (silica 0.48 NA and PCF 0.64 NA) were shown to be more sensitive to very tight bends of ≤ 80 mm diameter, where the output beam divergence would rapidly increase towards the NA of the fibre.

It can also be seen from figure 9 that the beam divergence from a straight length of fibre is very similar to that from a fibre with a 280 mm bend diameter. This implies that a fibre-delivered LI system can afford to have fibre bends as long as these are fairly large.

Of the three types of optical fibre tested, the sapphire was shown to be the least affected by bends in the fibre, with the exception of the 35 μm core PCF, which is evident from figure 10 for the 325 μm core diameter sapphire fibre of 0.12 NA. However, the minimum fibre bend diameter of the sapphire specified by the manufacturer (160 mm) was much larger than that of the other fibres, which were between 20 and 80 mm for the silica fibres.

Fibre bending was also found to affect the output beam intensity profile, as more modes were induced as the beam propagated through the fibre. This effect was more apparent for the higher NA fibres, which tended to produce an annular intensity profile as shown in figure 11. Moreover, all fibres were shown to be very sensitive at both input and output ends near the clamping point on the fibre connectors to small bends or 'kinks', which again typically resulted in an annular beam intensity profile.

Bending losses were evident from the fibre testing, although for the relatively larger fibre bend diameters (240 and 160 mm) these losses were quite low at around 1–2%, which has been shown in other research in the field [25]. However, beam transmission losses of up to 20% were found for the smallest permissible fibre bend diameters. These losses are due to the light rays inside the fibre exceeding the critical angle required for total internal reflection and escaping into the fibre

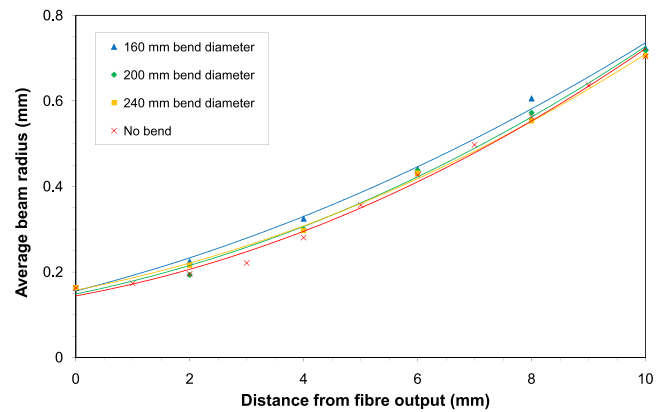


Figure 10. Output beam divergence from a 1 m length of 325 μm core diameter sapphire fibre of 0.12 NA with various bend diameters in the fibre.

cladding. Over time this was shown to lead to catastrophic failure at the point of the tight fibre bend.

One of the most interesting results of this study was from the effects of engine vibration on the output beam quality from the fibres. Engine vibration was found to increase the fibre output beam divergence angle as the engine was exciting the fibre, which constantly produced fibre bends. More interestingly, the extent of the divergence angle was shown to be dependent on the engine speed. The fibre output divergence angle varied disproportionately with increasing engine speed, where the greatest output beam angle was found at a particular engine speed which was different for each fibre tested. Here, the fibre output beam intensity profile changed from a typical multi-mode profile to a spiral pattern as illustrated in figure 12, which shows the output beam profiles from a 400 μm core 0.22 NA step index silica fibre at various output distances with and without engine vibration. This spiral mode pattern shown in figure 12 indicates that a possible resonant frequency of the 400 μm core fibre was found at an engine speed of 1500 rpm. These resonant effects are undesirable for a fibre-delivered LI system, as the fibre output beam quality is compromised. This led to the development of a rubber damping system, which was employed at both ends of the fibres on the clamping connector to retain the increased beam quality from using a shallow beam input angle and minimum twists and bends in the fibre. Although the fibre dampers were found to reduce the engine vibration effects on the fibre output beam, some beam quality was still lost in terms of increased output divergence.

3.4. Fibre-delivered LI engine testing

Of all the optical fibres tested offline, only four were really suitable for the online fibre-delivered LI engine tests. These were the silica step index 400 and 600 μm core diameters of both 0.12 and 0.22 NA. The focal lengths of the optical plug lenses for the 400 μm core fibres were 24 and 9 mm, which produced a minimum beam spot diameter of 150 μm . The focal lengths of the lenses used in the optical plug for the 600 μm core fibres were 30 and 9 mm, which produced a minimum beam spot diameter of 180 μm . The transmission

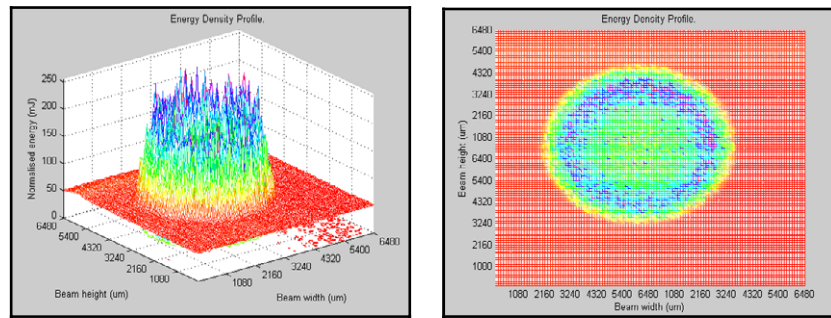


Figure 11. Fibre output annular beam intensity profile produced by small diameter bends along the fibre length.

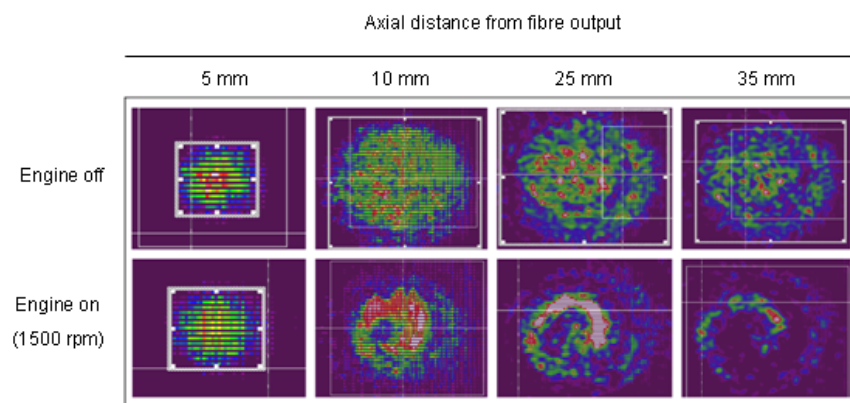


Figure 12. Cross-sectional beam intensity profiles at various distances from a 400 μm core 0.22 NA step index silica optical fibre output, with and without engine vibration.

of the overall optical system (fibre and optical plug) was measured to be $\approx 70\%$, which was mainly due to the uncoated optics and sapphire window. The focal point for both the optical plug configurations was at 4 mm from the end of the plug. This was found from previous research to be the optimum LI position for the test engine [1], which is also the same position of the electrical discharge of the engine spark plugs.

The optical plug was placed into cylinder 4 of the test engine, where the remaining three cylinders used conventional spark plugs. The spark timing for both fibre tests was at a crank angle of 20° before top dead centre. On starting up the engine, the laser input energy was set to nominal values of 10 and 20 mJ for the 400 and 600 μm core fibres, respectively, which was then ramped up to 50 and 65 mJ over the first 300 engine cycles. This was done to ensure that the fibre did not fail due to thermal shock from the high beam energies. Combustion data was collected in 300 engine cycle samples. Three fibre-delivered LI engine tests were performed on separate days for both the 400 and 600 μm core fibres. The data for these three tests were averaged and the results can be seen in figure 13. This shows the percentage of combustion events for the 400 and 600 μm core fibre-delivered LI tests in cylinder 4 only. It is evident that laser-induced combustion was achieved using fibre beam delivery, despite a relatively large percentage of misfires. It can be seen from figure 13 that the 600 μm core fibre LI tests produced a higher percentage of combustion events at around 35% average, compared with the 400 μm core

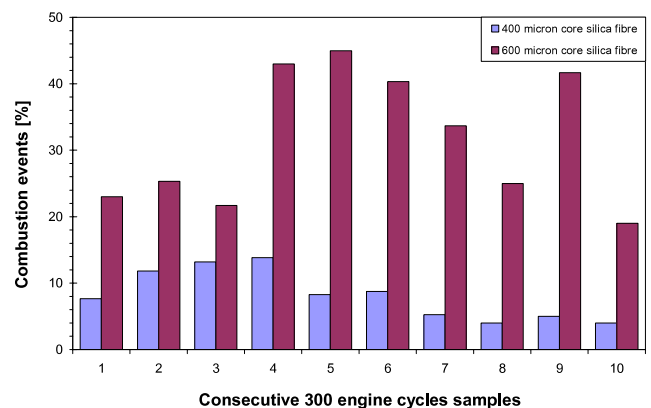


Figure 13. Percentage of combustion events for the 400 and 600 μm core fibre-delivered laser ignition tests in one cylinder of the test engine, where the three remaining cylinders were ignited by conventional spark plugs. Beam energies launched into the fibres were 50 and 65 mJ for the 400 and 600 μm core fibres, respectively.

fibre LI tests which produced about 8% average combustion. Looking at the results in figure 13, it may be logical to think that a fibre core size larger than 600 μm may give a higher percentage of combustion. However, the 600 μm fibre output beam divergence, when subjected to engine vibration, reached the diameter limitation inside the optical plug. Therefore, a beam from any larger core fibre would impinge on the inner walls of the optical plug, causing large transmission losses.

The self-cleaning mechanism in which the laser beam ablates combustion deposits from the optical plug window was shown to be present for the fibre-delivered LI engine tests. Observation of the optical plug window after engine testing showed a distinctive laser-irradiated spot in the deposited combustion residuals, which is shown in figure 14.

To further this research, the raw laser beam could be split into three separate equal beams, and individually coupled into three 600 μm core fibres. Then the fibre outputs could be combined and a specially designed diffractive optical element could be used to focus the three beams to one focal point. In theory this would effectively triple the deliverable beam energy to the cylinder and therefore achieve 100% combustion by fibre-delivered LI.

Damage thresholds for the fibres were found to be lower by about 20% for the online engine LI fibre-delivered tests, where the point of failure was typically at the connector clamping at the optical plug end of the fibre. This change in fibre failure point was most likely due to fatigue stress and heat build up caused by the running engine.

If fibre-delivered LI is to compete with spark plugs in the future, then the lifetime of the optical fibres should last at least 10 000 miles (~ 500 h) of operation. Therefore, the fibres must be able to withstand engine heat and vibration for prolonged hours of use. Moreover, the longevity of the optics within the optical plug (lenses and windows) should also be assured. Therefore, future studies in the field of LI should investigate the long term effects of these optical elements in a harsh IC engine environment, as there is insufficient research in this area.

4. Conclusion

The damage thresholds of the multi-mode silica step index were found to increase by employing the free-standing fibre ends in specially adapted fibre connectors, which lightly clamped the fibre at 100 mm from the ends. This allowed greater amounts of beam energy to be transmitted by the fibres, and hence larger laser irradiances at the focal point produced by the optical plug.

Fibre output beam divergence was found to decrease by reducing the beam input angle launched into the fibres, and therefore higher beam qualities could be obtained, meaning that the beam could be focused down to smaller spot sizes. However, in reducing the fibre beam input angle, the fibres became more susceptible to bending and engine vibration in terms of increased output divergence, reduced transmission and poorer beam mode quality.

In the fibre bending and vibration testing, the smaller numerical aperture fibres were found to be less susceptible compared to the higher numerical aperture fibres. The sapphire fibres were shown to be least affected by fibre bends and engine vibration. These bending and vibration effects on the fibre highlighted the need for a fibre damping mechanism in the fibre-delivered LI system.

Of all the fibres tested, the 400 and 600 μm core diameter silica step index fibres were shown to be the most suitable for single-fibre-beam-delivered LI, and were found to

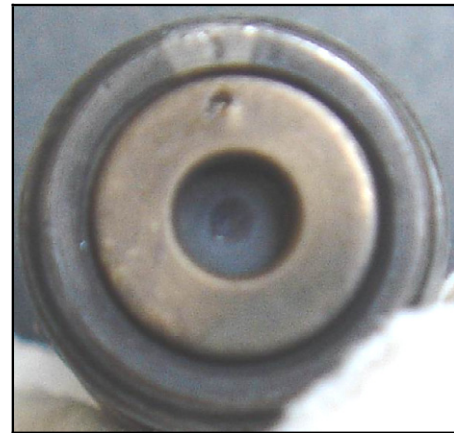


Figure 14. Optical plug end after fibre-delivered LI engine tests showing 'self-cleaned' area in the combustion deposits on the sapphire window.

produce combustion in the online testing, although not reliably. Nevertheless, the online tests demonstrated encouraging results for the realization of achieving 100% combustion with fibre beam delivery, where the possible next research step could be to multiplex a number of fibres together to increase the overall beam energy delivered to the engine cylinder. Furthermore, other types of fibres not included in this study, such as hollow core photonic bandgap fibres, should be investigated for application in LI, as there are many different cross sections of these fibres emerging which are increasingly being used to deliver high power laser beams. However, the beam energies currently needed for LI are somewhat higher than the damage threshold of these single-mode photonic bandgap fibres, and these would therefore need to be bundled or multiplexed in order to deliver adequate energy to initiate combustion of air/fuel mixtures.

Acknowledgments

The authors would like to thank John McCulloch for his technical assistance and expertise in manufacturing the optical plugs and other specialist components for this research. The authors also express their gratitude to Andy Scarisbrick, Stephan Carroll and Steve Keen for their support and encouragement in this study. Parts of this research were performed as a part of the LASIIC project consortium (University of Liverpool, Ford Motor Company and GSI Group) which was funded by the consortium and the Department of Trade and Industry (UK)—Foresight Vehicle Programme.

References

- [1] Dodd R, Mullett J D, Carroll S D, Dearden G, Shenton A T, Watkins K G, Triantos G and Keen S 2007 Laser ignition of an IC test engine using an Nd:YAG laser and the effect of key laser parameters on engine combustion performance *Lasers Eng.* **17** 213–31

- [2] Phuoc T X 2006 Laser-induced spark ignition fundamental and applications *Opt. Lasers Eng.* **44** 351–97
- [3] Phuoc T X 2000 Single-point versus multi-point laser ignition: experimental measurements of combustion times and pressures *Combust. Flame* **122** 508–10
- [4] Morsy M H and Chung S H 2003 Laser-induced multi-point ignition with a single-shot laser using two conical cavities for hydrogen/air mixture *Exp. Therm. Fluid Sci.* **27** 491–7
- [5] Mullett J D, Dodd D, Williams C J, Triantos G, Dearden G, Shenton A T, Watkins K G, Carroll S D, Scarisbrick A D and Keen S 2007 The influence of beam energy, mode and focal length on the control of laser ignition in an internal combustion engine *J. Phys. D: Appl. Phys.* **40** 4730–9
- [6] Mullett J D, Dickinson P B, Shenton A T, Dearden G and Watkins K G 2008 Multi-cylinder laser and spark ignition in an IC gasoline automotive engine: a comparative study *SAE Technical Paper* 2008-01-0470
- [7] Weinrotter M, Srivastava D K, Iskra K, Graf J, Kopecek H, Klausner J, Herdin G and Wintner E 2006 Laser ignition of engines: a realistic option! *Proc. SPIE* **6053** 605316
- [8] Ronney P D 1994 Laser versus conventional ignition of flames *Opt. Eng.* **33** 510–22
- [9] Chen Y L, Lewis J W L and Parigger C 2000 Spatial and temporal profiles of pulsed laser-induced air plasma emissions *J. Quant. Spectrosc. Radiat. Transfer* **67** 91–103
- [10] Bradley D, Sheppard C G W, Suardjaja I M and Woolley R 2004 Fundamentals of high-energy spark ignition with lasers *Combust. Flame* **138** 55–77
- [11] Kofler H, Tauer J, Tartar G, Iskra K, Klausner J, Herdin G and Wintner E 2007 An innovative solid-state laser for engine ignition *Laser Phys. Lett.* **4** 322–7
- [12] Joshi S, Yalin A P and Galvanauskas A 2007 Use of hollow core fibers, fiber lasers, and photonic crystal fibers for spark delivery and laser ignition in gases *Appl. Opt.* **46** 4057–64
- [13] Ramsden S A and Savic P 1964 A radiative detonation model for the development of a laser-induced spark in air *Nature* **203** 1217–9
- [14] Yalin A P, Defoort M, Willson B, Matsura Y and Miyagi Y 2005 Use of hollow core fibers to deliver nanosecond Nd:YAG laser pulses for spark formation *Opt. Lett.* **30** 2083–5
- [15] Matsuura Y, Hanamoto K, Sato S and Miyagi M 1998 Hollow fiber delivery of high-power pulsed Nd:YAG laser light *Opt. Lett.* **23** 1858–60
- [16] El-Rabii H and Gaborel G 2007 Laser ignition of flammable mixtures via a solid core optical fiber *Appl. Phys. B* **87** 139–44
- [17] Weinrotter M, Iskra K, Al-Janabi A H, Kopecek H and Wintner E 2005 Laser ignition of engines: multipoint, fiber delivery and diagnostics *Proc. SPIE* **5850** 88–98
- [18] Stakhiv A, Gilber R, Kopecek H, Zheltikov A M and Wintner E 2004 Laser ignition of engines via optical fibers? *Laser Phys.* **14** 738–47
- [19] Boechat A A P, Su D and Jones J D C 1992 Fibre optic beam delivery: launching efficiency measurement by dual-detector cladding power monitoring *Meas. Sci. Technol.* **3** 204–9
- [20] Sweatt W C, Setchell R E and Warren M E 1997 Injecting a pulsed YAG laser beam into a fiber *Proc. SPIE* **3010** 266–71
- [21] Allison S W, Gillies G T, Magnuson D W and Pagano T S 1985 Pulsed laser damage to optical fibres *Appl. Opt.* **24** 3140–5
- [22] Michaille L, Taylor D M, Bennett C R, Shepherd T J, Jacobsen C and Hansen T P 2004 Damage threshold and bending properties of photonic crystal and photonic band-gap optical fibres *Proc. SPIE* **5618** 30–8
- [23] Kuhn A, French P, Hand D P, Blewett I J, Richmond M and Jones J D C 2000 Preparation of fiber optics for the delivery of high-energy high-beam-quality Nd:YAG laser pulses *Appl. Opt.* **39** 6136–43
- [24] Kuhn A, Blewett I, Hand D P and Jones J D C 2000 Beam quality after propagation of Nd:YAG laser light through large core optical fibers *Appl. Opt.* **39** 6754–60
- [25] Boechat A A P, Su D, Hall D R and Jones J D C 1991 Bend loss in large core multimode optical fiber beam delivery systems *Appl. Opt.* **30** 321–7